Atmos. Chem. Phys., 9, 4315–4327, 2009
www.atmos-chem-phys.net/9/4315/2009/

Atmospheric Chemistry and Physics

Summertime impact of convective transport and lightning NO_x production over North America: modeling dependence on meteorological simulations

C. Zhao[1], Y. Wang[1], Y. Choi[2], and T. Zeng[1]

[1]School of Earth and Atmospheric Sciences, Georgia Institute of Technology, Atlanta, GA, USA
[2]Jet Propulsion Laboratory, Pasadena, CA, USA

Received: 10 December 2008 – Published in Atmos. Chem. Phys. Discuss.: 26 January 2009
Revised: 11 June 2009 – Accepted: 11 June 2009 – Published: 3 July 2009

Abstract. Global-scale chemical transport model simulations indicate lightning NO_x dominates upper tropospheric O_3 production above Eastern North America during summertime but vary in their estimates. To improve our understanding, a regional-scale model (REAM) with higher resolution is applied. To examine the uncertainties in modeling the impact of convective transport and lightning NO_x production on upper tropospheric chemical tracer distributions, REAM simulations of chemical tracers are driven by two meteorological models, WRF and MM5, with different cumulus convective parameterizations. The model simulations are evaluated using INTEX-A aircraft measurements and satellite measurements of NO_2 columns and cloud top pressure, and we find that mid and upper tropospheric trace gas concentrations are affected strongly by convection and lightning NO_x production. WRF with the KF-eta convection scheme simulates larger convective updraft mass fluxes below 150 hPa than MM5 with the Grell scheme. The inclusion of the entrainment and detrainment processes leads to more outflow in the mid troposphere in WRF than MM5. The ratio of C_2H_6/C_3H_8 is found to be a sensitive parameter to convective outflow; the simulation by WRF-REAM is in closer agreement with INTEX-A measurements than MM5-REAM, implying that convective mass fluxes by WRF are more realistic. WRF also simulates lower cloud top heights (10–12 km) than MM5 (up to 16 km), and hence smaller amounts of estimated (intra-cloud) lightning NO_x and lower emission altitudes. WRF simulated cloud top heights are in better agreement with GOES satellite measurements than MM5. Simulated lightning NO_x production difference (due primarily to cloud top height difference) is mostly above 12 km. At 8–12 km, the models simulate a contribution of 60–75% of NO_x and up to 20 ppbv of O_3 from lightning, although the decrease of lightning NO_x effect from the Southeast to Northeast and eastern Canada is overestimated. The model differences and biases found in this study reflect some major uncertainties of upper tropospheric NO_x and O_3 simulations driven by those in meteorological simulations and lightning parameterizations.

Correspondence to: C. Zhao
(chun.zhao@eas.gatech.edu)

1 Introduction

Tropospheric distributions of trace gases are driven in part by meteorological conditions. Convection and associated lightning NO_x production are two important meteorological processes affecting the production and distribution of tropospheric chemical tracers (e.g., Wang et al. 2001; Doherty et al. 2005; Hudman et al., 2007; Choi et al., 2005, 2008a). Convection redistributes trace gases vertically and significantly affects atmospheric chemical and transport processes during long-range transport (e.g., Wang et al., 2000, 2001; Doherty et al., 2005; Hess, 2005; Folkins et al., 2006; Kiley et al., 2006; Hudman et al., 2007). Li et al. (2005) and Choi et al. (2008b) showed the importance of convection in ventilating air pollutants from the continental boundary layer of the United States (US) and providing a conduit for US pollution to the Western North Atlantic Ocean.

Simulations of convective transport have large uncertainties. Several studies found substantial divergences among Chemical Transport Model (CTM) simulations arising from the difference in various cumulus parameterizations and underlying meteorological fields (e.g., Prather and Jacob, 1997; Prather et al., 2001; Collins et al., 2002; Doherty et al.,

2005). To properly evaluate model simulations of convective transport and lightning NO_x production, extensive atmospheric measurements are needed. One such dataset is the Intercontinental Chemical Transport Experiment – North America (INTEX-A) collected during summer (3 July to 15 August) 2004 over North America (Singh, et al., 2006), in which a large number of cases for active convection and large amounts of lightning NO_x production were measured (e.g., Hudman et al., 2007; Bertram et al., 2007).

Lightning is a major source of NO_x (NO_2+NO) in the upper troposphere. NO_x is thought to be produced during the return stroke stage of a cloud-to-ground flash and the leader stage of an intra-cloud flash but there remains a great deal of uncertainty in the mechanism of NO_x production in lightning flashes (e.g., Schumann and Huntrieser, 2007). The lightning flash rate is often parameterized as functions of meteorological variables such as convective updraft mass fluxes (UMF), convective available potential energy (CAPE), convective cloud top height, and precipitation rate (e.g., Price et al., 1993; Allen et al., 2000; Choi et al., 2005, 2008a). Lightning NO_x significantly enhances tropospheric NO_2 columns, in particular, over the ocean, where NO_2 columns are more sensitive to lightning NO_x production due to less impact of surface NO_x emissions (e.g., Choi et al. 2005, 2008a; Martin et al., 2006; Bertram et al., 2007). Cooper et al. (2009) presented a summary of many related observational and modeling studies over the US and suggested that lightning contributes to more than 80% of summertime NO_x in the upper troposphere in the region. It also increases the concentrations of O_3 and PAN in the free troposphere (e.g., Labrador et al., 2004; Cooper et al., 2006; Hudman et al., 2007). Hudman et al. (2007) found that lightning enhanced O_3 concentrations by 10–17 ppbv and PAN by 30% in the upper troposphere based on the INTEX-A measurements over Eastern North America and the Western North Atlantic Ocean during summer 2004 using the GEOS-CHEM model. Recent satellite measurements including NO_2 columns from the SCanning Imaging Absorption spectroMeter for Atmospheric CHartographY (SCIAMACHY) were used to show lightning enhanced NO_2 over the North Atlantic Ocean, and to constrain the global lightning NO_x emissions in the range of 4–8 Tg N/yr (Martin et al., 2006, 2007).

Previous analyses with global-scale models have shown difficulties in accurately quantifying the lightning-induced NO_x and O_3 production in the upper troposphere above North America during summer, as summarized by Cooper et al. (2009), with more recent estimates by Pfister et al. (2008) and Hudman et al. (2009). Simulated convective transport of tracers and lightning NO_x production are sensitive to underlying meteorological fields. To study the sensitivities in simulating their impact on trace gas simulations, we use a Regional chEmical trAnsport Model (REAM) with 70×70 km^2 resolution driven by two meteorological models with different convection schemes, the Weather Research and Forecasting (WRF) model (v3.0, Skamarock et al., 2005) with the KF-eta scheme (Kain, 2003) and the Fifth-Generation NCAR/Penn State Mesoscale Model (MM5) (v3.6.1, Grell et al., 1995) with the Grell scheme (Grell et al., 1993). When compared to the convective transport and lightning NO_x features measured during INTEX-A, the model difference between WRF-REAM and MM-5 REAM is attributed to the underlying meteorological fields, particularly the convection related variables.

Our analysis proceeds as follows. In Sect. 2, we describe the REAM model and the measurements used in the study. The convective impact on tropospheric tracers is analyzed in Sect. 3. The lightning impact is examined in Sect. 4. Conclusions are given in Sect. 5.

2 Model and observations

2.1 Model description

The REAM model driven by MM5 assimilated meteorological fields (MM5-REAM) was described by Choi et al. (2008a). Previously, this model was applied to investigate a number of tropospheric chemistry and transport problems at northern mid latitudes (Choi et al., 2005, 2008a, b; Jing et al., 2006; Wang et al., 2006; Gillus et al., 2008) and in the polar regions (Zeng et al., 2003, 2006; Wang et al., 2007). In this work, the REAM model is developed to use the WRF assimilated meteorological fields (WRF-REAM). Large changes are apparent in the free tropospheric chemical distributions when WRF fields are used in place of MM5.

The model has a horizontal resolution of 70 km with 23 vertical layers below 10 hPa. Meteorological fields are assimilated using either MM5 or WRF constrained by the NCEP reanalysis products (NNRP). The horizontal domain of MM5 or WRF has 5 extra grids beyond that of REAM on each side to minimize potential transport anomalies near the boundary. Most meteorological fields are archived every 30 min except those related to convective transport and lightning parameterizations (e.g., cloud top height, cloud base height, convective mass fluxes, and convection available potential energy CAPE), which are archived every 5 min. Chemical initial and boundary conditions for chemical tracers in REAM are obtained from the global simulation for the same period using the GEOS-CHEM model driven by GEOS-4 assimilated meteorological fields (Bey et al., 2001). Anthropogenic and biogenic emission algorithms and inventories are adapted from the GEOS-CHEM model (Choi et al., 2005, 2008a). One exception is that the emissions of NO_x, CO, and ($\geq C_4$ alkanes) over the US are prepared by Sparse Matrix Operator Kernel Emissions (SMOKE) model (http://cf.unc.edu/cep/empd/products/smoke/index.cfm) for 2004 projected from the Visibility Improvement State and Tribal Association of the Southeast (VISTAS) 2002 emission inventory, since we found that these emissions are more consistent with INTEX-A measurements than the default inventories

in GEOS-CHEM. Biomass burning emissions are included following Turquety et al. (2007). The default inventories in GEOS-Chem for ethane and propane are used since the ethane and propane emission ratios in the VISTAS inventory appear to be problematic, similar to the problem previously found by Wang et al. (1998).

Sub-grid convective transport in WRF-REAM and MM5-REAM is developed to be consistent with the KF-eta and Grell schemes implemented in WRF and MM5, respectively. The KF-eta scheme in WRF is developed based on the KF scheme (Kain and Fritsch, 1993). It utilizes a simple cloud model with moist updrafts and downdrafts, including the effects of detrainment and entrainment. Shallow convection is allowed for any updraft that does not reach minimum cloud depth for precipitating clouds; this minimum depth varies as a function of cloud-base temperature (Kain, 2003). The Grell scheme in MM5 is based on the rate of destabilization or quasi-equilibrium, a simple single-cloud scheme with updraft and downdraft fluxes and compensating motion determining the heating/moistening profile (Grell et al., 1993).

A newer and apparently quite different version of the Grell scheme (Grell and Devenyi, 2002) is available in the WRF model. Hence, the results shown in this study do not apply to the Grell scheme in WRF. We did not use the newer Grell (deep convection) scheme in WRF because there is no shallow convection scheme that can be paired with the Grell scheme in WRF, which is not the case in MM5. Shallow convection can be quite effective in ventilating pollutants from the boundary layer (e.g., Choi et al., 2005). A second reason is that MM5 with the Grell scheme has been widely used in previous regional chemical and transport modeling studies. Both KF-eta and (MM5) Grell convective schemes simulate moist updrafts and downdrafts. One notable difference is that the KF-eta scheme includes cloud entrainment and detrainment during convection but the Grell scheme does not. This difference is reflected in simulating the North America outflow of the pollutants and evaluated with INTEX-A measurements in this study.

The cloud-to-ground lightning flash rate is parameterized as a function of convective mass fluxes and CAPE on the basis of the observed cloud-to-ground lightning flashes by the National Lightning Detection Network (NLDN) in summer 2004 as described by Choi et al. (2005). The parameterization ensures the dynamic consistency between simulated lightning NO_x production and simualted convection events. The IC/CG flash ratio is calculated following Wang et al. (1998). It is assumed that IC and CG flashes have the same energy (Ott et al., 2003; Choi et al., 2005). Lightning NO_x is distributed vertically following the mid-latitude profile by Pickering et al. (1998). We set a NO_x production rate of 250 moles NO per flash in this study through trial and error analysis such that model simulations are consistent with in situ and satellite observations. This production rate happens to agree with the value suggested by Schumann and Huntrieser (2007).

2.2 Chemical observations

2.2.1 Aircraft observations

The Intercontinental Chemical Transport Experiment – North America Phase A (INTEX-A) was aimed at understanding the transport and transformation of gases and aerosols on transcontinental and intercontinental scales above Eastern North America (Singh et al., 2006). In this study, the INTEX-A measurements of C_2H_6, C_3H_8, HNO_3, NO, NO_2, and O_3 from the NASA DC-8 aircraft are used. C_2H_6 and C_3H_8 were measured with 1 pptv detection limit and 2–10% nominal accuracy (Simpson et al., 2000). HNO_3 was measured with 5–10 pptv detection limit and 10–15% nominal accuracy (Talbot et al., 1999; Crounse et al., 2006). NO was measured with a precision of 50 pptv with 1-min time integration (Ren et al., 2008). NO_2 was measured with 1 pptv detection limit and 10% nominal accuracy (Thornton et al., 2000). O_3 was measured with 1 ppbv detection limit and 5% nominal accuracy (Avery et al., 2001). All instruments on the DC-8 are described in detail by Singh et al. (2006). One-minute merge data of NO, NO_2, HNO_3, and O_3 and original data of C_2H_6 and C_3H_8 from DC-8 from July 1^{st} to 14 August 2004 are used (http://www-air.larc.nasa.gov/cgi-bin/arcstat). Some compounds were measured by two different techniques such as HNO_3. When both measurements are available, the average values are used. When we compare model simulations with measurements, the model output is sampled at the time and locations of in situ measurements.

2.2.2 Satellite measurements

Tropospheric NO_2 columns

The SCIAMACHY instrument onboard the ENVISAT satellite has a spatial resolution of $30\times60\,km^2$ and a 6-day global coverage. Tropospheric columns of NO_2 retrieved from SCIAMACHY and its uncertainties are calculated by Martin et al. (2006). The retrieval uncertainties are due to spectral fitting, the spectral artifact from the diffuser plate, removal of the stratospheric column, and air mass factor calculation. Measurements with cloud fraction greater than 30% are excluded in order to reduce the impact of clouds on the satellite retrievals. A more detailed description regarding the tropospheric NO_2 columns from SCIAMACHY and its validation with INTEX-A measurements can be found in Martin et al. (2006).

Cloud top pressure

The operational data collection phase of the International Satellite Cloud Climatology Project (ISCCP) began in July 1983 and the dataset provides a global cloud climatology based on the images from an international network of

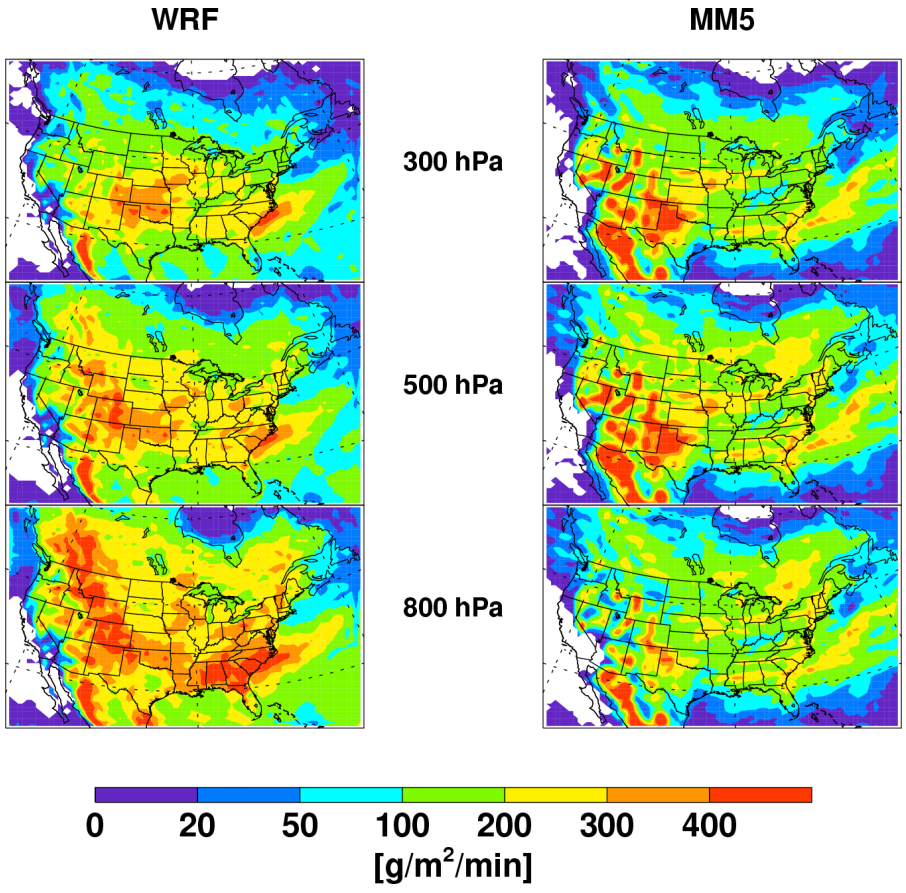

Fig. 1a. Mean deep convective updraft mass fluxes from WRF and MM5 simulations for July and August 2004.

weather satellites (Rossow and Schiffer, 1991). The measurements of cloud top pressure over North America provided by the ISCCP DX dataset with 3-hourly 30 km sampled pixels processed from the images of GOES-10 and GOES-12 satellites are used to evaluate the model simulated cumulus cloud top heights. The measurements with the cloud top pressure larger than 500 hPa are excluded in the study to filter out the low cloud information.

3 Sensitivities in modeling convective impact on tropospheric trace gases distributions

3.1 Dependence of convective transport on cumulus parameterization

Figure 1a shows the spatial distributions of the mean updraft mass fluxes of deep convection at three pressure levels (800, 500, and 300 hPa) from WRF and MM5 simulations with KF-eta and Grell convection schemes, respectively, for July and August 2004. WRF and MM5 simulate generally similar spatial distributions of mass fluxes with strong convection events over the Western and Southeastern US, Mexico, and the Western North Atlantic Ocean. One clear difference is that the updraft fluxes at 500 and 800 hPa are much higher in WRF than MM5. The mass fluxes in WRF are not as spatially concentrated over the Western-Central US and are greater over the Southeast than MM5. Figure 1b shows the vertical profiles of mass fluxes from the two models including the entrainment and detrainment fluxes only from WRF averaged over North America (domain shown in Fig. 1a). The difference is large. The updraft fluxes in WRF are much larger than MM5 at 300–900 hPa. The downdraft fluxes of WRF occur at lower altitudes than MM5. Entrainment and detrainment only in WRF are high in the lower and upper troposphere. The larger updraft fluxes as well as entrainment and detrainment in WRF lead to larger wet scavenging of soluble species than MM5. The convection top simulated by MM5 is higher than that by WRF. While the difference between MM5 and WRF simulated convective cloud top height is not that large in pressure coordinates, it is quite large in altitude coordinates, leading to a large difference in the distribution of pollutant outflow and lightning NO_x emissions.

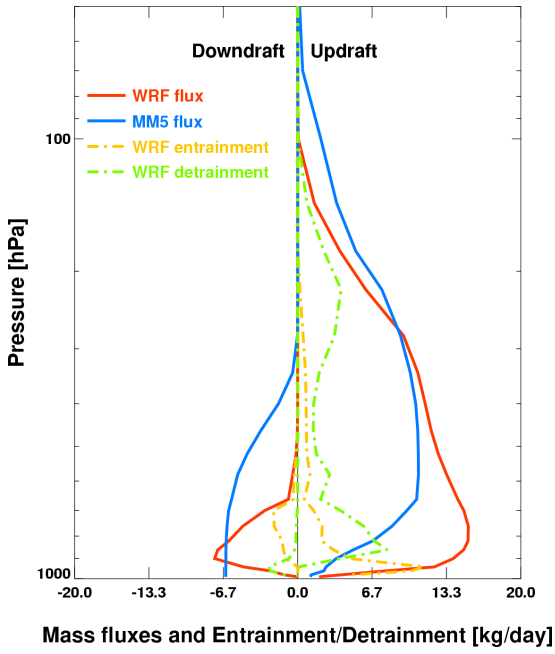

Fig. 1b. Vertical profiles of mean mass fluxes of deep convection from WRF and MM5 simulations, and the average entrainment and detrainment fluxes from the WRF simulation for July and August 2004 over North America (shown in Fig. 1a). Positive (negative) fluxes are updrafts (downdrafts).

3.2 Convective impact on export of pollutants

In the REAM model, convective transport lifts pollutants from the boundary layer into the free troposphere. As a result, concentrations increase at higher altitudes and decrease at lower altitudes. In model simulations, the change of concentrations as a function of altitude reflects the strength of convective transport. Here we use C_3H_8 as an example. Figure 2 shows the relative changes of C_3H_8 driven by convection at the surface and four pressure levels (800, 500, 300, and 150 hPa) for July and August 2004 in the two models. Both models show decreases of C_3H_8 at the surface and 800 hPa. At 500 hPa, convective transport increases C_3H_8 in WRF-REAM particularly over the Southeast because of entrainment and detrainment and updraft flux convergence. MM5-REAM, in contrast, shows a general convection-driven decrease. At higher altitudes, both models show increasing concentrations due to convection. However, the largest increase is at 300 hPa in WRF-REAM but at 150 hPa in MM5-REAM. The maximum outflow altitude is higher in MM5-REAM because the convective top is higher in MM5 (Fig. 1b).

The difference of the simulated C_2H_6 concentrations between the two models is within 10% (Appendix A). WRF-REAM simulated C_3H_8 concentrations are 10-30% higher than MM5-REAM in the free troposphere (3–8 km), in better agreement with the INTEX-A observations (Appendix A).

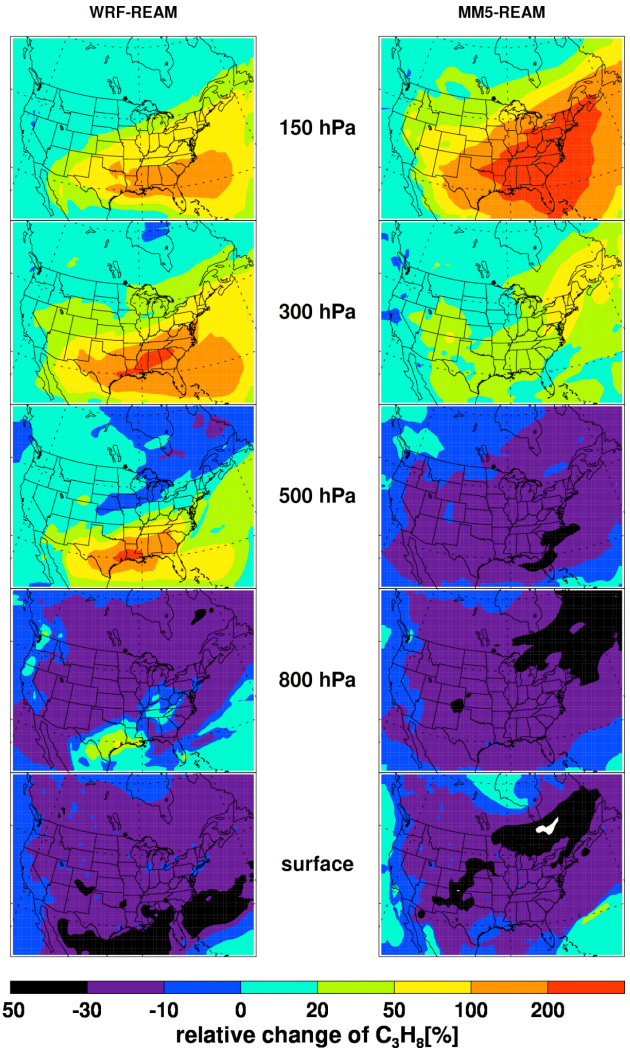

Fig. 2. Percentage changes of C_3H_8 in the standard model simulations from the model simulations without convective transport for July and August 2004 at the surface, and 150, 300, 500, and 800 hPa. Results for WRF-REAM and MM5-REAM are shown.

To minimize the effects of emission uncertainties and the large vertical gradient of C_2H_6 and C_3H_8 in this analysis, we investigate the convective effect on C_2H_6/C_3H_8 ratios (Wang and Zeng, 2004). The chemical lifetime of C_3H_8 (2 weeks) is shorter than C_2H_6 (>1 month). Long-range transport of C_3H_8 is less efficient and we expect to see a larger convective transport effect on C_3H_8 than C_2H_6.

We compare the median profiles of C_2H_6/C_3H_8 in both models with the INTEX-A measurements over the outflow region of the Western North Atlantic Ocean in Fig. 3. The measurements and corresponding simulated results are averaged into 1-km vertical bins. There are >50 measurements for each 1-km vertical bin. We also show the sensitivity results when convective transport is turned off in the models. The observations show the lowest median C_2H_6/C_3H_8 ratio

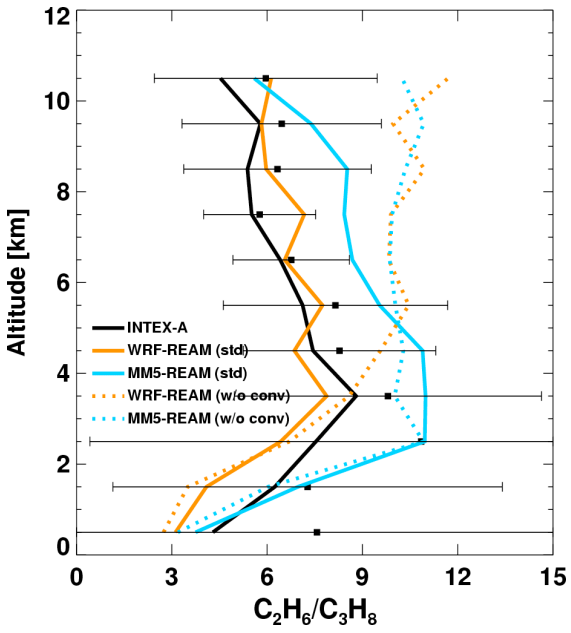

Fig. 3. Observed and simulated vertical profiles of median C_2H_6/C_3H_8 ratios in the outflow regions over the Western North Atlantic Ocean. There are >50 measurements for each 1-km interval. Black squares show the observed means at 1-km interval. The horizontal bars show the standard deviations. "std" denotes the standard simulation. "w/o conv" denotes the simulation where convective transport is turned off.

of 4–5 in the boundary layer. The observed ratio reaches a maximum of 9 at 3 km and gradually decreases to 4–5 at 11 km. Generally speaking, the ratio of C_2H_6/C_3H_8 increases in the troposphere as a result of differential chemical aging and atmospheric mixing (Wang and Zeng, 2004). Therefore, the ratio of C_2H_6/C_3H_8 tends to increase from the boundary layer to the free troposphere. The observed decrease of C_2H_6/C_3H_8 ratio reflects the effect of convective transport, which mixes upper tropospheric (high C_2H_6/C_3H_8 ratio) air masses with low C_2H_6/C_3H_8 ratio air masses lifted from the boundary layer into the free troposphere. We note that the amount of mixing is determined by flux vertical convergence, not by the direct fluxes shown in Fig. 1a. The measurement variability is larger in the lower troposphere, reflecting a mixture of fresh continental air with low C_2H_6/C_3H_8 ratios and aged marine air with high C_2H_6/C_3H_8 ratios over the Western North Atlantic Ocean.

Among the model simulations, both standard models reproduce the general profiles of the observed C_2H_6/C_3H_8 ratios; the profile from WRF-REAM is in closer agreement with the measurements. MM5-REAM median profile is at the upper bound of the measurements at 4–9 km. More telling of the model difference is in the sensitivity simulations. Without convective transport, the simulated median C_2H_6/C_3H_8 ratios in WRF-REAM would be a factor 2–3 too high compared to the measurements. In MM5-REAM, the effect of convective transport is evident only in the upper troposphere (above 7 km) as indicated in Fig. 2. The lack of convective mixing in MM5-REAM results in large overestimates of the C_2H_6/C_3H_8 ratios in the free troposphere at 3–9 km. The convective effect in MM5-REAM becomes larger than WRF-REAM above 11 km. There is no direct in situ observation to evaluate the model performance above 11 km. What we will show in Sect. 4.1 is that the convective cloud top is overestimated in MM5 compared with GOES satellite observations, particularly over the Western North Atlantic Ocean. WRF simulations are in closer agreement with the observations.

We also examine the effect of convective scavenging of soluble HNO_3. We assume that HNO_3 is removed in convective updrafts in the model (e.g., Wang et al., 2001). This wet scavenging pathway effectively removes HNO_3 lifted from the boundary layer. However, HNO_3 produced from lightning NO_x is not scavenged in this process. With entrainment (such as in WRF-REAM), background HNO_3 entrained into cumulus clouds is also removed. Without entrainment scavenging, upper tropospheric HNO_3 concentrations can be high from lightning NO_x. In general, simulated HNO_3 concentrations are lower in WRF-REAM than MM5-REAM and are in better agreement with the INTEX-A measurements although both model simulated median HNO_3 profiles are within the standard deviations of the measurements (Appendix A). WRF simulates larger convective mass fluxes than MM5 and also includes entrainment fluxes (Fig. 1b). Both factors contribute to larger wet scavenging in WRF-REAM.

4 Sensitivities in modeling lightning NO_x production

4.1 Cumulus cloud top and lightning NO_x production

We compare model simulated tropospheric NO_2 columns with SCIAMACHY measurements during INTEX-A period (1 July–15 August) (Martin et al., 2006) to illustrate the difference of lightning NO_x production between the two models (Fig. 4). The temporal resolution of SCIAMACHY is low, covering the globe every 6 days. After filtering out measurements with cloud fractions >30%, there are only about 2 days of measurements per model grid over most regions of the Eastern US during INTEX-A period; on average, there are 3 days of measurements over the US. Therefore, the comparison here is qualitative in nature. Some of the overestimates in the models can be traced back to simulated lightning influence during one of the measurement days. WRF-REAM and MM5-REAM simulations are very similar when lightning NO_x is excluded. When including lightning NO_x, WRF-REAM simulated NO_2 columns are lower than MM5-REAM and are closer to the limited observations. The spatial correlation is also higher in WRF-REAM (R=0.73) than MM5-REAM (R=0.58). Lightning

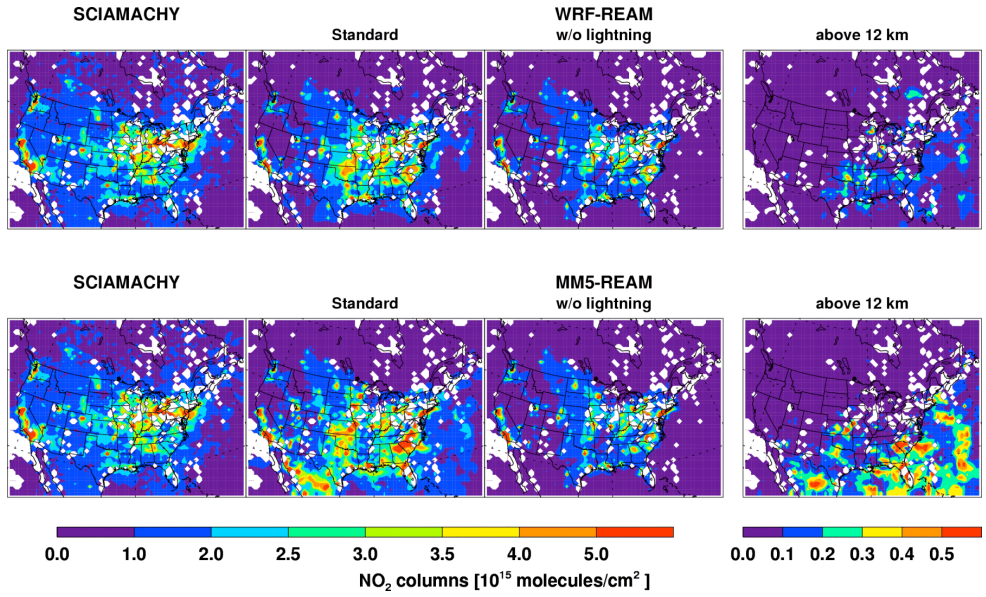

Fig. 4. Tropospheric NO_2 columns derived from SCIAMACHY measurements (Martin et al., 2006) and simulated by WRF-REAM and MM5-REAM during the INTEX-A period (1 July to 15 August 2004). Tropospheric NO_2 columns from the standard simulation and a sensitivity simulation without lightning NO_x are shown. Also shown are the tropospheric columns above 12 km in the standard simulation. Only the measurements with cloud fractions <30% and the corresponding simulation results are used. White areas indicate that no measurement data are available.

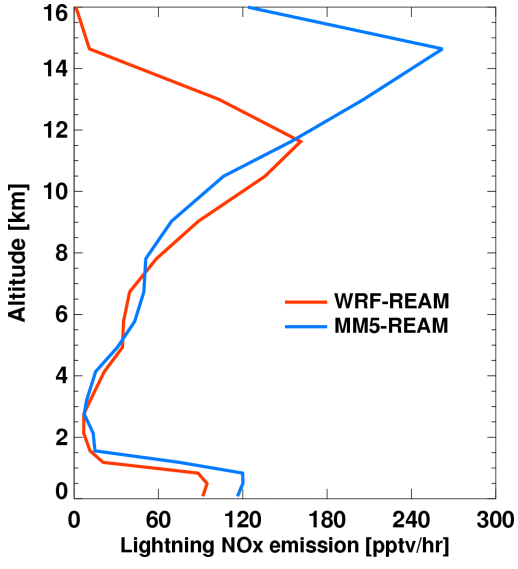

Fig. 5. Mean lightning NO_x production rate profiles in WRF-REAM and MM5-REAM for 1 July–15 August 2004 averaged over the INTEX-A region.

NO_x concentrations are lower in WRF-REAM than MM5-REAM. For example, NO_2 columns above 12 km are mainly due to lightning NO_x. They are much lower in WRF-REAM than in MM5-REAM (Fig. 4). Over the Western North Atlantic Ocean, NO_2 columns above 12 km account for 10% of the total columns in WRF-REAM but ∼50% in MM5-REAM. Specifying a lower NO_x production rate per flash in MM5-REAM than WRF-REAM can correct the high bias in MM5-REAM. However, the correction will also lead to large underestimations in MM5-REAM compared to INTEX-A aircraft measurements (to be discussed in the next section).

The large difference in simulated lightning NO_x production between WRF-REAM and MM5-REAM is due mainly to the difference in the simulated cumulus cloud top heights. The simulated vertical distribution of lightning NO_x in both models follows the mid-latitude profile by Pickering et al. (1998). Figure 5 shows the vertical distributions of lightning NO_x production in the two models averaged over the INTEX-A regions. MM5-REAM simulates the lightning NO_x maximum at ∼15 km much higher than that in WRF-REAM at ∼12 km. It is important to note that even though MM5-REAM simulates much more total lightning NO_x than WRF-REAM, the two models simulate similar lightning NO_x production at 2–12 km, which will explain why they simulate similar lightning impact on the upper tropospheric (8–12 km) NO_2 and O_3 concentrations shown in the next section. Our lightning NO_x parameterization is based on the observed cloud-to-ground (CG) flash rates from the NLDN network (Choi et al., 2005, 2008a). The intra-cloud (IC) lightning flash rates are estimated in the model as a function of the freezing altitude and cumulus cloud top height (Wang et al., 1998). A higher cloud top height generally leads to higher lightning NO_x production.

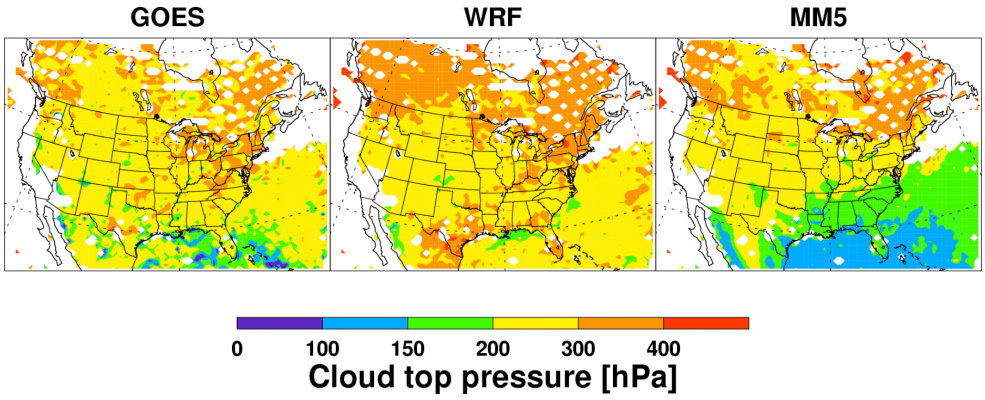

Fig. 6. Mean cumulus cloud top pressures measured by GOE-10 and GOE-12 satellites and simulated by WRF and MM5 for 1 July–15 August 2004. Measurement data >500 hPa (and corresponding model results) are excluded to filter out the low cloud information.

We therefore evaluate model simulated cumulus cloud top heights with the measurements by GOES-10 and GOES-12 satellites from the DX cloud dataset of the ISCCP (Rossow and Schiffer, 1991) in Fig. 6. Clearly, the problem is in MM5 results, where cloud top pressures are underestimated over most regions of the Gulf of Mexico, the southeastern US and the Western North Atlantic Ocean. An exception is over Southern Florida, where MM5 simulated cloud top heights are more consistent with the observations than WRF, which may indicate that the entrainment and detrainment are overestimated in WRF over that region. The overestimates of cloud top heights lead to higher IC/CG flash ratios and overestimates of lightning NO_x production in these regions (Fig. 4). The average IC/CG flash ratio over the US from WRF-REAM is 5, much lower than that of 7 from MM5-REAM during the INTEX-A period. It also becomes apparent that lightning NO_x in MM5-REAM is injected too high in altitude (Fig. 5). Convection in WRF with the KF-eta scheme extends to a lower altitude of 10–12 km, rather than up to 16 km in MM5 with the Grell scheme. Satellite measurements of NO_2 (indirectly) and cloud top pressure (directly) indicate that cloud top height simulated by WRF is more realistic.

4.2 Effect of lightning NO_x during INTEX-A

The large model difference in lightning NO_x is not necessarily reflected in the comparison with aircraft NO_x measurements because the flight ceiling of the DC-8 is 12 km. Figure 7 shows the comparisons of upper tropospheric NO_x at 8–12 km along the DC-8 flight tracks. The difference between WRF-REAM and MM5-REAM is not as significant as we found in Fig. 4–6 because of the similar lightning NO_x emissions from the two models at 2–12 km (Fig. 5). Upper tropospheric NO_x in both models are driven by lightning, which increases NO_x mixing ratios by a factor of up to 5 (~500 pptv). Both models simulate larger lightning impact over the South Eastern US than over the Northeast and Eastern Canada. Measurements indicate that the model underestimates lightning NO_x production in the latter regions.

Figure 8 shows the comparison of the latitudinal distribution of upper tropospheric NO_x (8-12 km) over Eastern North America (25° N–55° N and <90° W). Generally, both models significantly underestimate lightning NO_x over the regions north than 35° N. MM5-REAM overestimates NO_x concentrations over the southeastern US due in part to the subsidence of large amounts of lightning NO_x above 12 km (Fig. 5). Both models simulate that NO_x concentrations decrease by a factor of >5 from the Southeast to the Northeast and Eastern Canada, much larger than a factor of 2 or less in the measurements. Similar large biases in the simulated south-to-north decrease of lightning NO_x over Eastern North America can also be found in previous studies (e.g., Li et al., 2005; Hudman et al., 2007; Cooper et al., 2006 and 2009). Figure 1a shows that convective mass fluxes in the upper troposphere in both WRF and MM5 are generally low over the Northeast. Measurements by the NLDN network also show low CG flashes there. Therefore, the model underestimate may reflect that the lightning parameterization should be formulated differently over the northern regions from southern regions of Eastern North America.

Lightning NO_x is a major source of O_3 in the upper troposphere and significantly affects the budget of tropospheric O_3. Hudman et al. (2007, 2009) found lightning can increase upper troposphere O_3 concentrations by 10–17 ppbv and Cooper et al. (2006) found an increase of 11–13 ppbv on average and suggested a maximum of 24 ppbv based on the box model analysis during INTEX-A over the Eastern US. We find, here, that O_3 concentrations are increased by up to ~20 ppbv (Fig. 7) over the region and the average O_3 enhancement is ~10 ppbv over the region. The results are in line with previous studies. Despite the difference in the underlying meteorological fields, simulated O_3 concentrations and their sensitivities to lightning NO_x are similar between WRF-REAM and MM5-REAM since lightning

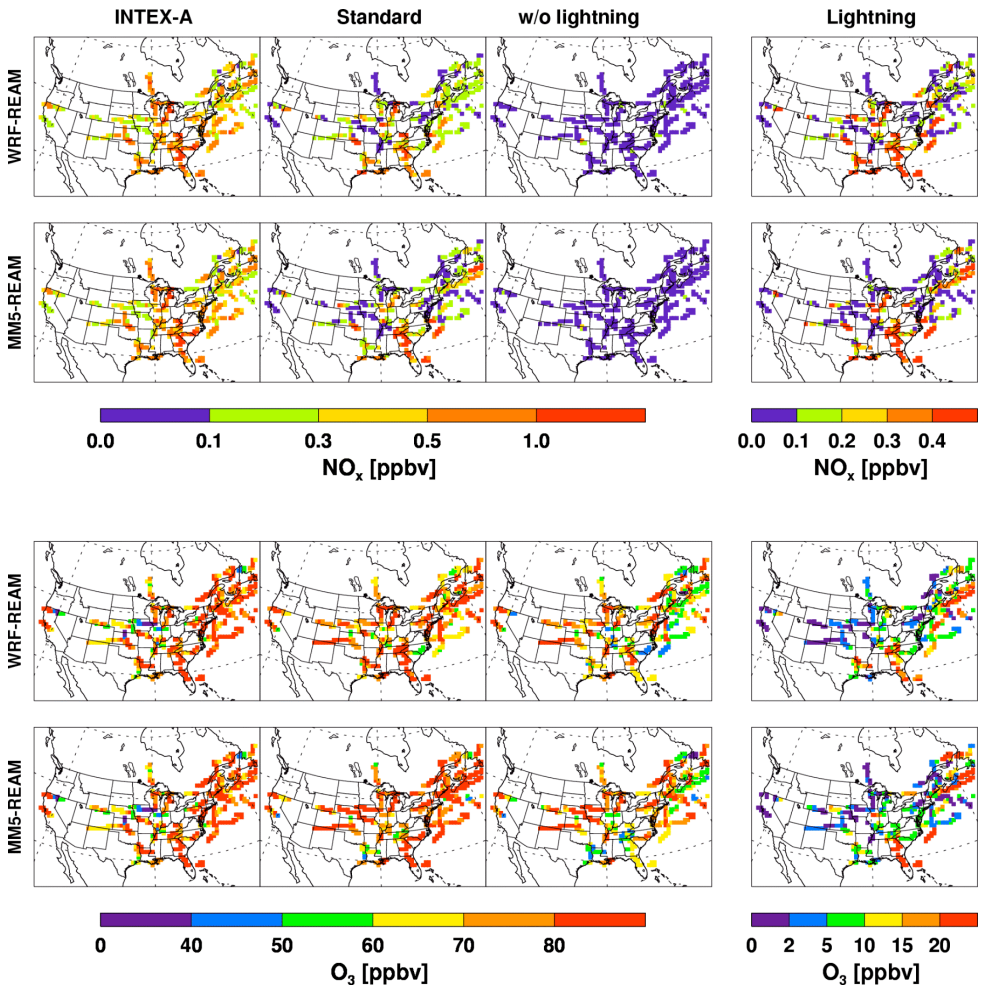

Fig. 7. Observed and simulated upper tropospheric NOx and O_3 concentrations along DC-8 flight tracks at 8–12 km during the INTEX-A experiment. Results from the standard simulations and sensitivity simulations without lightning NO_x using WRF-REAM and MM5-REAM are shown. The impacts of lightning (rightmost column) are estimated by subtracting the sensitivity results from the standard model results.

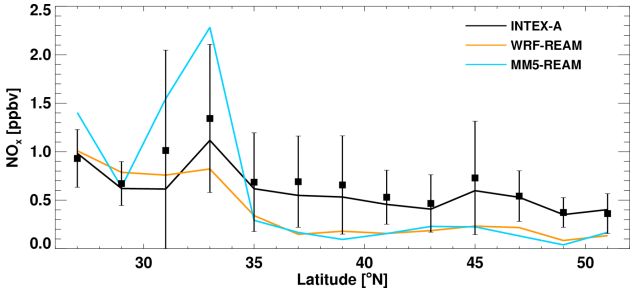

Fig. 8. Observed and simulated latitudinal distributions of median upper tropospheric NO_x (8–12 km) over Eastern North America (25° N–55° N and <90° W). There are >20 measurements for each 2° latitude band. Black squares show the observed means and the vertical bars show the standard deviations.

enhancements of NO_x are similar between the two models at 8–12 km. The enhancements of O_3 by lightning NO_x improve model simulations compared to INTEX-A measurements. Upper tropospheric O_3 concentrations are affected by lightning mainly over the southeastern US and eastern Canada. Tropospheric O_3 production from surface emissions of NO_x and volatile organic compounds (VOCs) and transport from the stratosphere also make significant contributions to upper tropospheric O_3 (Choi et al., 2008a).

4.3 Relative contributions of surface and lightning emissions to tropospheric NO_x

The relative importance of the different odd nitrogen sources in the troposphere, particularly lightning NO_x, over the US has been investigated in previous studies (e.g., Cooper et al., 2009, and the references therein). We use WRF-REAM and MM5-REAM to estimate the lightning and

surface NO_x contributions over the INTEX-A regions (covering the US and Western North Atlantic Ocean) from 1 July–15 August. In our simulations, WRF-REAM and MM5-REAM show similar results up to 12 km. Lightning contribution to NO_x increases from ∼10% in the boundary layer to 60–75% at 8–12 km. In contrast, the surface emission contributions decrease from 80% in the boundary layer to ∼10% at 8–12 km. Our estimation of lighting contribution is smaller than that of 80–95% by Cooper et al. (2009), although they found some evidence for model overestimation of lightning NO_x over the Southeast and our simulations have a clear low bias compared to INTEX-A measurements over the Northeast and Eastern Canada (Fig. 7).

Above 12 km, the two models clearly diverge. WRF-REAM and MM5-REAM calculate, ∼50% and ∼90% of the NO_x are due to lightning, respectively. The NO_x concentrations at 12–15 km from the MM5-REAM simulation are more than double those from the WRF-REAM simulation due to lightning. The divergence between WRF-REAM and MM5-REAM above 12 km reflects the lightning NO_x vertical profiles in Fig. 4. The NO_x mixing ratios due to surface emissions in the MM5-REAM simulation are ∼50% greater than those from the WRF-REAM simulation because of the absence of dilution from entrainment and detrainment and the higher cloud top height in MM5 simulation.

We also estimate the source contributions to total reactive nitrogen (NO_y) at 8–12 km. Both models suggest contributions of ∼40 and 10% to NO_y from lightning and surface emissions over North America at 8–12 km, respectively. Previously, Allen et al. (2000) estimated that 13% and 16% are due to lightning and surface emissions over North America for October–November 1997 during the SONEX Experiment, respectively. More intensive summertime lightning is likely the reason for a larger lightning impact in our results.

5 Conclusions

REAM driven by two meteorological models, WRF (WRF-REAM) and MM5 (MM5-REAM) with different convective schemes, is used to evaluate the model sensitivities in convective transport and lightning NO_x production to meteorological simulations. When compared to the convective transport and lightning NO_x features measured during INTEX-A, we find that simulated convective transport and lightning NO_x production are very sensitive to the difference of the underlying meteorological fields particularly the variables directly affected by the cumulus convection scheme.

WRF with the KF-eta scheme simulates larger updrafts from the lower troposphere, resulting in significantly more outflow at 3–9 km than MM5 with the Grell scheme. A sensitivity chemical indicator affected by this outflow is the C_2H_6/C_3H_8 ratio. While WRF-REAM shows large decreases (up to a factor of 2) of the C_2H_6/C_3H_8 ratio at 3–9 km due to convective outflow, the change is relatively small in MM5-REAM. In comparison, the two model results are in agreement in the boundary layer and 10–11 km. WRF-REAM simulations are clearly in closer agreement with the INTEX-A observations. Larger mass fluxes as well as entrainment and detrainment in WRF-REAM also lead to more scavenging of soluble HNO_3 in the free troposphere than MM5-REAM. The simulated median profile of HNO_3 by WRF-REAM is in closer agreement with the measurements than MM5-REAM, although the observed variation is larger than the model difference.

WRF with the KF-eta scheme simulates lower convective cloud top heights than MM5 with the Grell scheme. The cloud top height directly affects the model estimates of intra-cloud lightning production. Consequently, WRF-REAM simulates less lightning NO_x than MM5-REAM and the maximum lightning NO_x altitude of 12 km in WRF-REAM is lower than 15 km in MM5-REAM. Measurements of tropospheric NO_2 columns from SCIAMACHY provide a qualitative comparison, which suggests that WRF-REAM is closer to the observations, although the lower temporal resolution and cloud presence over convective regions greatly reduced the number of valid measurements. Evaluation using the ISCCP cloud top height measurements from GOES satellites clearly demonstrated that MM5 simulated convective cloud tops are too high over the southeastern US and the Western North Atlantic Ocean.

We note that the large model difference in lightning NO_x production occurs mostly above 12 km, where no in situ measurements were available from INTEX-A. For future field missions targeting the effect of lightning NO_x and convective transport, observations above 12 km are needed.

Despite the large differences discussed previously, the two models show similar agreement with upper tropospheric in situ NO_x measurements. Over the observation regions of INTEX-A, the two models show consistent results for the effect of lightning NO_x in the upper troposphere (8–12 km): (1) lightning enhances upper tropospheric NO_x concentrations by up to a factor of >5 (∼500 pptv) and NO_2 columns by a factor of >1.5 over the ocean; (2) lightning and surface emissions over North America contribute to NO_x (NO_y) at 8–12 km by 60–75% (40%) and ∼10% (10%), respectively; and (3) lightning NO_x increases O_3 concentrations by up to 20 ppbv with an average of 10 ppbv. These results are generally consistent with previous studies conducted with coarser resolution global models.

A major model bias is that the decrease of lightning NO_x effect (at 8–12 km) from the Southeast to the Northeast and Eastern Canada is significantly overestimated. Inspections of previous modeling results show similar biases. This model bias results from lesser convective activities simulated by both MM5 and WRF and lesser cloud-to-ground lightning flash rates in the observations. The bias indicates a need for a different lightning parameterization for the Southeast from the Northeast and eastern Canada. The model uncertainties driven by meteorological fields and lightning

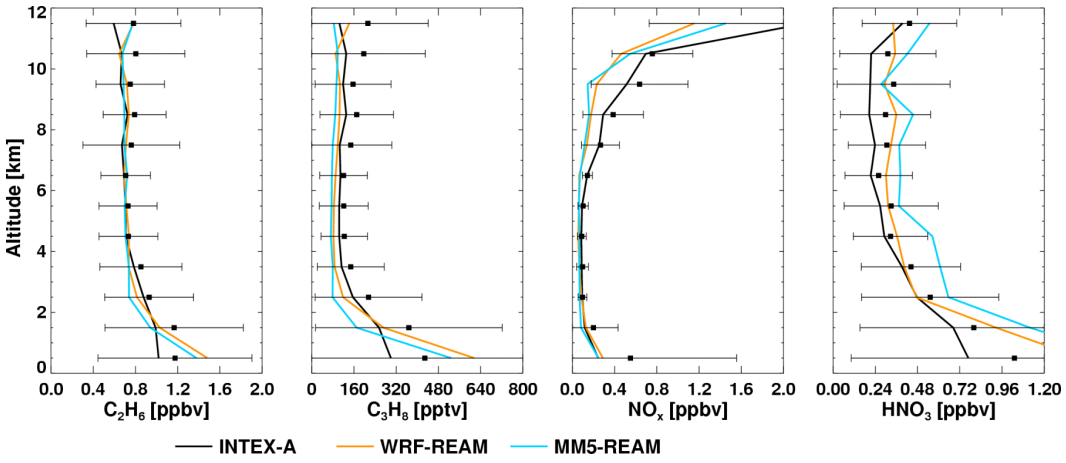

Fig. A1 Observed and simulated vertical profiles of median C_2H_6, C_3H_8, NO_x, and HNO_3 over the INTEX-A region on 1 July–15 August, 2004. Black squares show the observed means and the horizontal bars show the standard deviations. There are >200 data points for each 1-km interval.

parameterizations found in this study are implicit in all previous studies of upper tropospheric NO_x and O_3. For proper model-to-model (and model-to-observation) comparisons, key meteorological fields such as cloud top height and parameters such as IC/CG ratio need to be documented clearly in future studies.

Appendix A

REAM model evaluations with INTEX-A measurements

The evaluation here largely follows that by Hudman et al. (2007). Figure A1 compares the simulated and observed vertical distributions of C_2H_6, C_3H_8, NO_x, and HNO_3 concentrations during INTEX-A. The measurements and corresponding model results are averaged into 1-km vertical bins. There are >200 measurements for each 1-km vertical bin. The model successfully reproduces the observed concentrations of the C_2H_6 and C_3H_8 in the free troposphere. The difference of simulated C_2H_6 between WRF-REAM and MM5-REAM is within 10%. WRF-REAM simulates 10–30% higher C_3H_8 concentrations than MM5-REAM in the free troposphere (3–8 km). Both models overestimate the lower tropospheric C_2H_6 and C_3H_8 concentrations, likely resulting from the uncertainties of their emissions. The comparison over the outflow region of the Western Atlantic Ocean is similar.

REAM simulated vertical NO_x profiles are similar to the GEOS-CHEM result shown by Hudman et al. (2007). The observed NO_x profile by Hudman et al. (2007) is lower than shown here or that by Cooper et al. (2009); the reason is unclear. The observed C-shape profile is simulated by REAM. The upper tropospheric NO_x is underestimated. Figure 7 and 8 shows that most of the underestimation is over the Northeast and Eastern Canada. Increasing the lightning NO_x production rate per flash in the model would lead to an overestimation over the Southeast and cause a large bias compared to satellite observed tropospheric NO_2 columns (Fig. 4). WRF-REAM and MM5-REAM simulated NO_x profiles from the surface to 12 km are similar.

HNO_3 is generally well simulated by both WRF-REAM and MM5-REAM in the free troposphere but overestimated in the boundary layer. WRF-REAM simulated 15-35% less HNO_3 concentrations in the free troposphere than MM5-REAM, in closer agreement to the measurements.

Acknowledgements. We thank Randall Martin for providing satellite retrieval data and Kenneth Cummins for providing the NLDN effective detection efficiency. We thank the NASA Tropospheric Chemistry Program and the investigators (M. Avery, D. Blake, B. Brune, R. Cohen, R. Talbot, and P. Wennberg) for making available the INTEX-A measurements we used in this study. This paper benefited from extensive comments and suggestions by Owen Cooper and two anonymous reviewers. The GEOS-CHEM model is managed at Harvard University with support from the NASA Atmospheric Chemistry Modeling and Analysis Program. This work was supported by the National Science Foundation Atmospheric Chemistry program.

Edited by: O. Cooper

References

Allen, D. J., Pickering, K. E., Stenchikov, G., Thompson, A., and Kondo, Y.: A three-dimensional total odd nitrogen (NO_y) simulations during SONEX using a stretched-grid chemical transport model, J. Geophys. Res., 105, 3851, doi:10.1029/2002JD002066, 2000.

Avery, M. A., Westberg, D. J., Fuelberg, H. E., Newell, R. E., Anderson, B. E., Vay, S. A., Sachse, G., and Blake, D. R.: Chemical transport across the ITCZ in the central Pacific during and El Nino-Southern Oscillation cold phase event in March–April 1999, J. Geophys. Res., 106, 32539–32553, 2001.

Bey, I., Jacob, D. J., Yantosca, R. M., Logan, J. A., Field, B. D., Fiore, A. M., Li, Q., Liu, H., Mickley, L. J., and Schultz, M. G.: Global modeling of tropospheric chemistry with assimilated meteorology: Model description and evaluation, J. Geophys. Res., 106, 23073–23096, 2001.

Bertram, T. H., Perring, A. E., Wooldridge, P. J., Crounse, J. D., Kwan, A. J., Wennberg, P. O., Scheuer, E., Dibb, J., Avery, M., Sachse, G., Vay, S. A., Crawford, J. H., McNaughton, C. S., Clarke, A., Pickering, K. E., Fuelberg, H., Huey, G., Blake, D. R., Singh, H. B., Hall, S. R., Shetter, R. E., Fried, A., Heikes, B. G., and Cohen, R. C.: Direct Measurements of the Convective Recycling of the Upper Troposphere, Science, 315, 816–820, 2007.

Choi, Y., Wang, Y., Zeng, T., Martin, R. V., Kurosu, T. P., and Chance, K.: Evidence of lightning NO_x and convective transport of pollutants in satellite observations over North America, Geophys. Res. Lett., 32, L02805, doi:10.1029/2004GL021436, 2005.

Choi, Y., Wang, Y., Zeng, T., Cunnold, D., Yang, E., Martin, R., Chance, K., Thouret, V., and Edgerton, E.: Springtime transitions of NO_2, CO, and O_3 over North America: Model evaluation and analysis, J. Geophys. Res., 113, D20311, doi:10.1029/2007JD009632, 2008a.

Choi, Y., Wang, Y., Yang, Q., Cunnold, D., Zeng, T., Shim, C., Luo, M., Eldering, A., Bucsela, E., and Gleanson, J.: Spring to summer northward migration of high O_3 over the western North Atlantic, Geophys. Res. Lett., 35, L04818, doi:10.1029/2007GL032276, 2008b.

Collins, W. J., Derwent, R. G., Johnson, C. E., and Stevenson, D. S.: A comparison of two schemes for the convective transport of chemical species in a Lagrangian global chemistry model, Q. J. Roy. Meteor. Soc., 128, 991–1009, 2002.

Cooper, O. R., Stohl, A., Trainer, M., Thompson, A. M., Witte, J. C., Oltmans, S. J., et al.: Large upper tropospheric ozone enhancements above midlatitude North America during summer: In situ evidence from the IONS and MOZAIC ozone measurement network, J. Geophys. Res., 111, D24S05, doi:10.1029/2006JD007306, 2006.

Cooper, O. R., Eckhardt, S., Crawford, J. H., Brown, C. C., Cohen, R. C., Bertram, T. H., Wooldridge, P., Perring, A., Brune, W. H., et al.: Summertime buildup and decay of lightning NO_x and aged thunderstorm outflow above North America, J. Geophys. Res., 114, D01101, doi:10.1029/2008JD010293, 2009.

Crounse, J. D., K. A. Mckinney, A. J. Kwan, and P. O. Wennberg: Measurement of gas-phase hydroperoxides by chemical ionization mass spectrometry, Anal. Chem., 78, 6726–6732, 2006.

Doherty, R. M., Stevenson, D. S., Collins, W. J., and Sanderson, M. G.: Influence of convective transport on tropospheric ozone and its precursors in a chemistry-climate model, Atmos. Chem. Phys., 5, 3205–3218, 2005.

Folkins, I., Bernath, P., Boone, C., Donner, L. J., Eldering, A., Lesins, G., Martin, R. V., Sinnhuber, B. M., and Walker, K.: Testing convective parameterizations with tropical measurements of HNO_3, CO, H_2O, and O_3: Implications for the water vapor budget, Geophys. Res. Lett., 111, D23304, doi:10.1029/2006JD007325, 2006.

Grell, G. A.: Prognostic evaluation of assumptions used by cumulus parameterizations, Mon. Weather Rev., 121, 764–787, 1993.

Grell, G. A.: A description of the fifth-generation Penn State/NCAR mesoscale model (MM5), NCAR Tech. Note, June, 1995.

Grell, G. A. and Devenyi, D.: A generalized approach to parameterizing convection combining ensemble and data assimilation techniques, Geophys. Res. Lett., 29, 1693, doi: 10.1029/2002GL015311, 2002.

Guillas, S., Bao, J., Choi, Y., Wang, Y., Khaing, H., Nesbit, C., and Huey, G.: downscaling of chemical transport ozone forecasts over Atlanta, Atmos. Environ., 42, 1338–1348, 2008.

Hess, P. G.: A comparison of two paradigms: The relative global roles of moist convective versus nonconvective transport, J. Geophys. Res., 110, D20302, doi:10.1029/2004JD005456, 2005.

Hudman, R. C., Jacob, D. J., Turquety, S., Leibensperger, E. M., Murray, L. T., Wu, S., Gilliland, A. B., Avery, M., Bertram, T. H., Brune, W., Cohen, R. C., Dibb, J. E., Flocke, F. M., Fried, A., Holloway, J., Neuman, J. A., Orville, R., Perring, A., Ren, X., Ryerson, T. B., Sachse, G. W., Singh, H. B., Swanson, A., and Wooldridge, P. J.: Surface and lightning sources of nitrogen oxides over the United States: magnitudes, chemical evolution, and outflow, J. Geophys. Res., 112, D12S05, doi:10.1029/2006JD007912, 2007.

Hudman, R. C., Murray, L. T., Jacob, D. J., Turquety, S., Wu, S., Millet, D. B., Avery, M., Goldstein, A. H., and Holloway, J.: North American influence on tropospheric ozone and the effects of recent emission reductions: Constraints from ICARTT observations, J. Geophys. Res., 114, D07302, doi:10.1029/2008JD010126, 2009.

Jing, P., Cunnold, D., Choi, Y., and Wang, Y.: Summertime tropospheric ozone columns from Aura OMI/MLS measurements versus regional model results over the United States, Geophys. Res. Lett., 33, L17817, doi:10.1029/2006GL026473, 2006.

Kain, J. S.: The Kain-Fritsch Convective Parameterization: An Update, J. Appl. Meteo., 43, 170–181, doi:10.1175/1520-0450(2004)043, 2003.

Kain, J. S. and J. M. Fritsch: Convective parameterization for mesoscale models: The Kain-Fritsch scheme, The Representation of cumulus convection in numberical models, Meteor. Monogr., Amer. Meteor. Soc., 24, 165–170, 1993

Kiley, C. M. and Fuelberg, H. E.: An examination of summertime cyclone transport processes during Intercontinental Chemical Transport Experiment (INTEX-A), J. Geophys. Res., 111, D24S06, doi:10.1029/2006JD007115, 2006.

Labrador, L., Kuhlmann, R. V., and Lawrence, M. G.: Strong sensitivity of the global mean OH concentration and the troposphere's oxidizing efficiency to the source of NO_x from lightning, Geophys. Res. Lett., 31, L06102, doi:10.1029/2003GL019229, 2004.

Labrador, L. J., Kuhlmann, R. V., and Lawrence, M. G.: The effects of lightning-produced NO_x and its vertical distribution on atmospheric chemistry: sensitivity simulations with MATCH-MPIC, Atmos. Chem. Phys., 5, 1815–1834, 2005.

Li, Q., Jacob, D. J., Park, R., Wang, Y., Heald, C. L., and Hudman, R.: North American pollution outflow and the trapping of convectively lifted pollution by upper-level anticyclone, J. Geophys. Res., 110, D10301, doi:10.1029/2004JD005039, 2005.

Martin, R. V., Sioris, C. E., Chance, K., Ryerson, T. B., Bertram, T. H., Wooldridge, P. J., Cohen, R. C., Neuman, J. A., Swanson,

A., and Flocke, F. M.: Evaluation of space-based constraints on global nitrogen oxide emissions with regional aircraft measurements over and downwind of Eastern North America, J. Geophys. Res., 111, D15308, doi:10.1029/2005JD006680, 2006.

Martin, R. V., Sauvage, B., Folkins, I., Sioris, C. E., Boone, C. Bernath, P., and Ziemke, J.: Space-based constraints on the production of nitric oxide by lightning, J. Geophys. Res., 112, D09309, doi:10.1029/2006JD007831, 2007.

Ott, L. E., Pickering, K., Stenchikov, G., Lin, R., Ridley, B., Lopez, J., Loewenstain, M., and Richard, E.: Trace gas transport and lightning NO_x production during a CRYSTAL-FACE thunderstorm simulated using a 3-D cloud-scale chemical transport model, Eos Trans. AGU, 84(46), Fall Meet. Suppl., Abstract AE32A-0156, 2003.

Pfister, G. G., Emmons, L. K., Hess, J. F., Thompson, A. M., and Yorks, J. E.: Analysis of the summer 2004 ozone budget over the United States using Intercontinental Transport Experiment Ozonesonde Network Study (IONS) observations and Model of Ozone and Related Tracers (MOZART-4) simulations, J. Geophys, Res., 113, D23306, doi:10.1029/2008JD010190, 2008.

Pickering, K. E., Wang, Y., Tao, W., Price, C., and Muller, J.: Vertical distributions of lightning NO_x for use in regional and global chemical transport models, J. Geophys. Res., 103, 31202–31216, 1998.

Prather, M. J. and Jacob, D. J.: A persistent imbalance in HO_x and NO_x photochemistry of the upper troposphere driven by deep tropical convection, Geophys. Res. Lett., 24, 3189–3192, 1997.

Prather, M. J.: Atmospheric Chemistry and Greenhouse Gases, in: Climate Change 2001: The Scientific Basis, Contribution of WG1 to the Third Assessment report of the IPCC, edited by: Houghton, J. T., Ding, Y., Griggs, D. J., Noguer, M., et al., Cambridge University Press, UK, 2001.

Price, C. and Rind, D.: What determines the cloud-to-ground lightning fraction in thunderstorms?, J. Geophys. Res., 98, 463–466, 1993.

Ren, X., Olson, J. R., Crawford, J. H., Brune, W. H., Mao, J., Long, R. B., Chen, Z., Chen, G., Avery, M. A., Sachse, G. W., Barrick, J. D., Diskin, G. S., Huey, L. G., Fried, A., Cohen, R. C., Heikes, B., Wennberg, P. O., Singh, H. B., Blake, D. R., and Shetter, R. E.: HO_x chemistry during INTEX-A 2004: Observation, model calculation, and comparison with previous studies, J. Geophys. Res., 113, D05310, doi:10.1029/2007JD009166, 2008.

Rossow, R. W. and Schiffer, R. A.: ISCCP cloud data products, B. Am. Meteor. Soc., 72, 2–20, 1991.

Schumann, U. and Huntrieser, H.: The global lightning-induced nitrogen oxides source, Atmos. Chem. Phys., 7, 3823–3907, 2007, http://www.atmos-chem-phys.net/7/3823/2007/.

Simpson, I. J., Sive, B. C., Blake, D. R., Blake, N. J., Chen, T. Y., Lopez, J. P., Anderson, B. E., Sachse, G. W., Vay, S. A., Fuelberg, H. E., Kondo, Y., Thompson, A. M., and Rowland, F. S.: Nonmethane hydrocarbon measurements in the North Atlantic Flight Corridor during the Subsonic Assessment Ozone and Nitrogen Oxide Experiment, J. Geophys. Res., 105, 3785–3793, 2000.

Singh, H. B., Brune, W. H., Crawford, J. H., Jacob, D. J., and Russell, P. B.: Overview of the summer 2004 Intercontinental Chemical Transport Experiment-North America (INTEX-A), J. Geophys. Res., 111, D24S01, doi:10.1029/2006JD007905, 2006.

Singh, H. B., Salas, L., Herlth, D., Kolyer, R., Czech, E., Avery, M., Crawford, J. H., Pierce, R. B., Sachse, G. W., Blake, D. R., Cohen, R. C., Bertram, T. H., Perring, A., Wooldridge, P. J., Dibb, J., Huey, G., Hudman, R. C., Turquety, S., Emmons, L. K., Flocke, F., Tang, Y., Carmichael, G. R., and Horowitz, L. W.: Reactive nitrogen distribution and partitioning in the North American troposphere and lowermost stratosphere, J. Geophys. Res., 111, D12S04, doi:10.1029/2006JD007664, 2007.

Skamarock, W. C., Klemp, J. B., Dudhia, J., Gill, D. O., Barker, D. M., Wang, W., and Powers, J. G.: A Description of the Advanced Research WRF Version 2, NCAR Tech. Note, June, 2005.

Thornton, J. A., Wooldridge, P. J., and Cohen, R. C.: Atmospheric NO_2: In situ laser-induced fluorescence detection at parts per trillion mixing ratios, Anal. Chem., 72, 528–539, 2000.

Talbot, R. W., Dibb, J. E., Scheuer, E. M., Kondo, Y., Koike, M., Singh, H. B., Salas, L. B., Fukui, Y., Ballenthin, J. O., Meads, R. F., Miller, T. M., Hunton, D. E., Viggiano, A. A., Blake, D. R., Blake, N. J., Atlas, E., Flocke, F., Jacob, D. J., and Jeagle, L.: Reactive Nitrogen budge during the NASA SONEX mission, Geophys. Res. Lett., 26, 3057–3060, 1999.

Turquety, S., Logan, J. A., Jacob, D. J., Hudman, R. C., Leung, F. Y., Heald, C. L., Yantosca, R. M., Wu, S., and Emmons, L. K.: Inventory of boreal fire emissions for North America in 2004: Importance of peat burning and pyroconvective injection, J. Geophys. Res., 112, D12S03, doi:10.1029/2006JD007281, 2007.

Wang, Y., Jacob, D. J., and Logan, J. A.: Global simulation of tropospheric O_3-NO_x-hydrocarbon chemistry: 1. Formulation, J. Geophys. Res., 103, 10713–10725, 1998.

Wang, Y., Liu, S. C., Yu, H., and Sandholm, S. T.: Influence of convection and biomass burning on tropospheric chemistry over the tropical Pacific, J. Geophys. Res., 105, 9321–9333, 2000.

Wang, Y., Liu, S. C., Wine, P. H., Davis, D. D., Sandholm, S. T., Atlas, E. L, Avery, M. A., Blake, D. R., Blake, N. J., Brune, W. H., Heikes, B. G., Sachse, G. W., Shetter, R. E., Singh, H. B., Talbot, R. W., and Tan, D.: Factors controlling tropospheric O_3, OH, NO_x, and SO_2 over the tropical Pacific during PEM-Tropics B, J. Geophys. Res., 106, 32733–32747, 2001.

Wang, Y., and Zeng, T.: On tracer correlations in the troposphere: The case of ethane and propane, J. Geophys. Res., 109, D24306, doi:10.1029/2004JD005023, 2004.

Wang, Y., Choi, Y., Zeng, T., Ridley, B., Blake, N., Blake, D., and Flocke, F.: Late-spring increase of trans-Pacific pollution transport in the upper troposphere, Geophys. Res. Lett., 33, L01811, doi:10.1029/2005GL024975, 2006.

Wang, Y., Choi, Y., Zeng, T., Davis, D., Buhr, M., Huey, G., and Neff, W.: Assessing the photochemical impact of snow NO_x emissions over Antarctica during ANTCI 2003, Atmos. Environ., 41, 3944–3958, 2007.

Zeng, T., Wang, Y., Chance, K., Browell, E. V., Ridley, B. A., and Atlas, E. L.: Widespread persistent near-surface ozone depletion at northern high latitudes in spring, Geophys. Res. Lett., 30(24), 2298, doi:10.1029/2003GL018587, 2003.

Zeng, T., Wang, Y., Chance, K., Blake, N., Blake, D., and Ridley, B.: Halogen-driven low altitude O_3 and hydrocarbon losses in spring at northern high latitudes, J. Geophys. Res., 111, D17313, doi:10.1029/2005JD006706, 2006.